Molecular Vision 2003; 9:538-48 <http://www.molvis.org/molvis/v9/a66>
Received 23 June 2003 | Accepted 18 September 2003 | Published 7 October 2003

Gene expression profiling in human age-related nuclear cataract

Roberta Ruotolo,[1] Francesca Grassi,[2] Riccardo Percudani,[1] Claudio Rivetti,[1] Davide Martorana,[3] Giovanni Maraini,[2] Simone Ottonello[1]

[1]Dipartimento di Biochimica e Biologia Molecolare, University of Parma, Parma, Italy; [2]Dipartimento di Scienze Otorino Odonto Oftalmologiche e Cervico Facciali, University of Parma, Parma, Italy; [3]Dipartimento di Clinica Medica, Nefrologia e Scienze della Prevenzione, University of Parma, Parma, Italy

Purpose: To identify genes that are differentially expressed in age-related nuclear cataracts compared to transparent human lenses.
Methods: Total RNA was extracted from pools of central 5 mm capsulorrhexis epithelial samples microdissected at surgery from eyes with nuclear cataract or from age-matched transparent lenses (post-mortem). mRNA levels in the two samples were compared by hybridization to DNA microarrays (GeneFilter GF211) containing 4,132 known human genes. Only mRNAs consistently modulated over four comparisons were retained for analysis. A subset of the mRNA expression differences thus identified were verified and confirmed by Real-Time RT-PCR. Expressed and modulated genes were categorized according to the Gene Ontology classification.
Results: The data revealed 262 genes that are downregulated and 7 that are upregulated by a factor of 2.5 or more in epithelial samples from cataractous lenses compared with transparent lenses. The highest content of downregulated genes was found in the functional classes "Signal transduction", "Regulation of cell proliferation", and "Protein modification". The "Response to oxidative stress" class was one of the least modulated. Among downregulated genes, we found several mRNAs coding for transcription/translation-related proteins, heat shock proteins 70 and 27, two ubiquitin-conjugating enzymes, two subunits of the cytoskeletal/chaperone protein, tubulin, βA4-crystallin, and a group of Alzheimer-related proteins, including presenilin 1 and presenilin 2.
Conclusions: An extensive mRNA downregulation accompanies the development of the nuclear type of human age-related cataract. A few genes and classes of genes more prominently displaying this type of response have been identified. Altogether, the data indicate the tendency, in age-related nuclear cataract, towards a shutdown of de novo RNA and protein biosynthesis rather than an upregulation of cell defense components such as chaperones and various kinds of antioxidative or detoxifying proteins.

Age-related cataract still represents the most frequent worldwide cause of visual impairment and, frequently, of blindness. Even though much is known about the environmental cues and biochemical changes associated with age-related loss of lens transparency, the sequence of events ultimately leading to cataract formation is far from being elucidated. One of the most popular hypotheses considers oxidative stress as a possible cause of age-related cataract, and evidence derived from in vitro analyses as well as from cataractous human eyes studies have been supportive of this possibility [1-3]. Other studies, however, came up with inconclusive or even negative results as to a critical involvement of oxidative stress in cataractogenesis [4]. The same is largely true for observational studies aimed at evaluating a possible role of the anti-oxidant status of human participants in preventing (or at least delaying) the development of age-related lens opacities [5-7].

The identification of genes differentially expressed in age-related cataract compared with transparent adult human lenses is likely to provide important insights into the metabolic and protective processes that characterize the tissue response to the disease. Although the overall spectrum of gene modulation that characterizes the development of lens opacification is presently largely unknown, some information has been gained recently both in animal models of age-onset cataract and in the human age-related disease. RT-PCR differential display analysis of lens mRNAs has resulted in the identification of a limited number of transcripts that appear to be up- or down-regulated in the lens epithelium of human lenses with age-related cataract (or corresponding animal disease models) as compared to epithelial samples from normal transparent lenses [8-11]. In the Emory mouse, a well-characterized model of age-dependent cataract, Sheets et al. [8] reported the downregulation of αA- and βA3/A1-crystallin and the upregulation of the ARK receptor tyrosine kinase. In human lens epithelium derived from age-related cataracts, Kantorow et al. [9-11] observed abnormal changes in the expression levels of a few transcripts, including increased expression of metallothionein IIA and osteonectin, and decreased expression of the protein Phosphatase 2A regulatory subunit, as well as of the mRNAs for ribosomal proteins L21, L15, L13a, and L7a.

A more comprehensive picture of the mRNA expression profile of a tissue and of the changes in expression levels that can take place during disease development (or maintenance, as in late onset chronic diseases such as age-related cataract) may be obtained with the use of DNA microarrays, a tech-

Correspondence to: Giovanni Maraini, Ophthalmology, University of Parma, Via Gramsci 14, 43100 Parma, Italy; Phone: +39 0521 703098; FAX: +39 0521 994820; email: maraini@unipr.it

nique that allows the simultaneous analysis of thousands of genes within a single test [12]. To our knowledge, no microarray analysis of human cataract has been reported so far. We have utilized microarrays containing 4,132 human cDNAs of known function to compare the mRNA expression profiles of human lens central epithelium samples obtained at surgery from pure nuclear age-related cataracts with those of central lens epithelial samples surgically microdissected from adult transparent human lenses. The main outcome of this study is that a fairly extensive downregulation (affecting more than 40% of the 612 genes in our array that turned out to be expressed in the lens) is the main gene expression change associated with the development of age-related cataract in man. A few functional classes of genes more prominently display this type of response. A general resemblance between cataract and other age-related diseases (most notably Alzheimer) has been identified.

METHODS

Isolation of epithelium-capsule samples from human lenses: A few days before surgery, cataractous lenses were classified for type and severity of the opacity at the slit-lamp by an experienced observer according to LOCS II [13]. Only lenses with a nuclear opalescence grade greater than or equal to 2 and a cortical and/or posterior sub-capsular opacity grade less than or equal to 1 were selected for the present study. Written informed consent was obtained and the principles of the Declaration of Helsinki were observed during this study. Epithelium-capsule samples (approximately 5 mm in diameter) obtained immediately after capsulorrhexis in the operating room were carefully washed to eliminate possible contamination by blood and fiber cells, and immediately stored at -80 °C. Two pools of cataractous epithelial tags (64% females) were thus set up (pool 1: n=14, mean age 75 ±7.5 years; pool 2: n=14, mean age 75.3 ±6.7 years) and utilized for the preparation of two distinct cDNA probes that were employed for two independent microarray hybridization experiments (see below). A single pool of normal lens epithelia (n=14, 52% females) was set up from adult donors (mean age 62.9 ±8.9 years) with the same surgical technique under an operating microscope during multi-organ explant procedures. Epithelial lens tags were obtained immediately after corneal removal, which was usually the last of the multi-organ explants to be performed. The time elapsed between the interruption of mechanical ventilation and ocular explant was thus always less than one h, except for one case in which the interval was 6 h. Only epithelia from transparent lenses having no sign of opacity were collected.

RNA extraction and probe preparation: Total RNA was prepared from epithelial tag pools using the RNAzol B extraction method (Biotech Italia, Roma, Italy) according to the manufacturer's recommendations, except for a final 4 M LiCl precipitation that was followed by an ethanol wash of the pellet and by an additional sodium acetate/ethanol precipitation. The amount of RNA in each sample was quantified by both spectrophotometric analysis and gel-electrophoresis, followed by analysis of ethidium bromide-stained gels with the Quantity One software (BioRad, Hercules, CA). Radioactively labelled, single-stranded cDNA probes were produced by reverse-transcription (90 min at 37 °C) of total RNA (2 μg) in reaction mixtures containing 2.0 μg of oligo-$dT_{16\text{-}18}$, 6 μl of 5X first-strand buffer, 1.5 μl of reverse transcriptase (Superscript II, Invitrogen, Paisley, UK), 1.5 μl of a dNTP mixture containing dATP, dGTP, dTTP (each at a 20 mM concentration), and 250 μCi of [^{33}P]-dCTP (2,500 Ci/mmol; Amersham Biosciences Corp, Piscataway, NJ). The resulting cDNA probes were purified on Bio-Spin 6 columns (BioRad) and quantified using a scintillation counter.

Microarray hybridization: Human "Named Genes" GeneFilters Microarrays (GF211, Release 1), consisting of 4,132 cDNAs (IMAGE consortium collection, greater than or equal to 1 kbp in length) coding for proteins of known function, spotted onto nylon membranes (Invitrogen, Carlsbad, CA), were used for hybridization analysis according to the manufacturer's instructions (Research Genetics Invitrogen Corporation, Gene Filters® Mammalian Microarrays Technical Handbook). Filters were prehybridized with 5.0 μg of denatured Cot-1 DNA, 5.0 μg of poly-dA and 4 ml of MicroHyb hybridization solution (Invitrogen) for 2 h at 42 °C, followed by the addition of radiolabeled probes and hybridization for 18 h at 42 °C. After a double-wash at 50 °C with 2X SSC, 1% sodium dodecyl sulfate (SDS, 20 min each), plus a 15 min wash at 55 °C (0.5X SSC, 1% SDS), membranes were aligned on a phosphorimaging screen (Super Resolution SR, PerkinElmer, Branchburg, NJ), wrapped with a lead envelope, and exposed for various lengths of time at room temperature. The screens were scanned with a Cyclone phosphorimager (PerkinElmer) at a resolution of 42 μm and saved as digital images using the OptiQuant software. Two GF211 filters from different batches (hereby designated F1 and F2) were separately hybridized with radiolabeled cDNA probes containing the same amount of incorporated [^{33}P]-dCMP radioactivity. Probes designated C1 and C2 were prepared from RNA samples extracted from two different cataractous epithelial tag pools (a biological replicate carried out with pools 1 and 2, see above). Two cDNA probes, independently prepared from RNA derived from a single pool of transparent epithelial tags (designated N1 and N2, a technical replicate), were utilized for "normal lens" hybridizations. N1 and C1, and N2 and C2

Table 1. Concordant spots from two independent sets of pairwise hybridizations

	Above background regular spots (flag 0)	Above background irregular spots (flag 3)	Background level spots (flag 2)
N-probe hybridization	348	264	2,988
C-probe hybridization	92	91	3,224

Data refer to the total number of concordantly flagged spots obtained from independent N1 versus N2 and C1 versus C2 hybridizations carried out on filter 1 (N1 and C1) or 2 (N2 and C2). The total number of non-concordant spots was 532 and 725, for N-probe and C-probe hybridizations, respectively. Spots tagged as flag 3 in at least one of the two hybridizations (N1 versus N2, or C1 versus C2) are included in this flag pair class.

were hybridized with filters 1 and 2, respectively. Filters were utilized no more than three-times. Prior to re-utilization they were stripped in hot 0.5% SDS for 1 h.

Data analysis: Digitized images of comparable overall signal intensity as measured with the program Quantity One (BioRad) were used for hybridization analysis. Individual images, as well as various pairwise combinations (N versus N, C versus C, and N versus C, n=6), were initially analyzed with the GF211-dedicated software Pathways 4 (Invitrogen). A more detailed, and quantitatively rigorous analysis was then performed with the program ImaGene 5.0 (Biodiscovery, Marina Del Rey, CA). For each spot, the program calculates the mean signal and the mean local background intensity. Spots with a signal intensity (Is) exceeding local background intensity (Ib) by at least one standard deviation of the mean local background measured across the entire array are tagged by the program as flag 0. For each of such spots, the hybridization intensity (Is-Ib) was calculated and normalized with respect to the mean of all the hybridization intensities of flag 0 spots. Spots with a signal intensity differing from the local background by less than one standard deviation of the background measured across the entire array are tagged by the program as flag 2. These spots were by far the most abundant and were regarded as background level. When required (eg, for the determination of an arbitrary expression ratio in an N versus C comparison) they were assigned an intensity value corresponding to the minimum normalized intensity in that particular hybridization. Spots with a local background differing from the background distribution measured across the entire image and/or with an irregular shape are tagged as flag 3. These included some of the most strongly hybridizing cDNAs in the entire array (see Results). Therefore, cDNAs corresponding to flag 3 spots were assigned an average local background. Normalization was performed by considering the mean intensity of all above-background spots. Spots flagged as 0/0, 0/3, 3/0, or 3/3 in two independent N versus N (or C versus C) hybridizations were deemed as "concordant" and representative of expressed genes. By the same criterion, concordant flag 2 spots were considered as representative of non-expressed genes. The total number of concordant spots obtained from four independent hybridizations carried out with the N and the C probes is reported in Table 1. Concordance between hybridizations performed on filter 1 and filter 2 was estimated, in pairwise comparisons, from the percentage of concordant spots over the total number of cDNAs. It was 87% and 83% for N1 versus N2 and C1 versus C2, respectively, and a lower overall hybridization intensity was consistently observed with filter 2. For N versus C comparisons (N=4), data analysis was conducted on hybridizations performed with the same filter (N1 versus C1 and N2 versus C2) as well as across filters (N1 versus C2 and N2 versus C1). Spots labeled as flag 0, 3, or 2 in N and 0 or 3 in C, with a normalized signal intensity ratio (I_C/I_N) greater than or equal to 1.5 were judged as upregulated in C. Spots labeled as flag 0 or 3 in N and 0, 3, or 2 in C, with an (I_N/I_C) greater than or equal to 1.5 were judged as downregulated in C. Only spots with an average signal intensity ratio greater than or equal to 2.5 were considered as representative of modulated mRNAs. Genes were categorized according to GeneOntology [14]. Functional classification of genes was carried out with the DAVID program [15]. Statistical analysis of gene distribution in the different functional

Table 2. Primer sequences, sizes and melting temperatures for Real-Time PCR amplicons

Target gene	Primer sequence	Amplicon length (bp)	Tm (°C)
Crystallin βA4	For.: 5'-GAAGTGCTGAGTGGAGCGTG-3' Rev.: 5'-CCTTGGAAGCCAGCATGCT-3'	51	80
Glucosidase 1	For.: 5'-CCTCACGTCTACTTCGGCATGA-3' Rev.: 5'-CCACATCAGTCCGGTGAGGA-3'	63	82
Gelsolin	For.: 5'-GAAGACCTGGCAACGGATGA-3' Rev.: 5'-TGAGAATCCTTTCCAACCCAGA-3'	77	81
Presenilin 1	For.: 5'-GCTCAGGAGAGAAATGAAACGC-3' Rev.: 5'-CCTTCTGCCATATTCACCAACC-3'	80	76
Polymerase (RNA) II polypeptide E	For.: 5'-GTCCCTGAGCACGTCGTCAT-3' Rev.: 5'-GGCAGCTGGTTCTCTCGGA-3'	80	83
Dhydropyrimidinase-like 2	For.: 5'-GGACCCCGACAGCGTTAAA-3' Rev.: 5'-GGCACTCCATGCCTTCAAAG-3'	83	80
β-2-microglobulin	For.: 5'-GTATGCCTGCCGTGTGAACC-3' Rev.: 5'-CCCTCCATGATGCTGCTTACAT-3'	86	80

The Tm of each amplicon was determined by melting curve analysis.

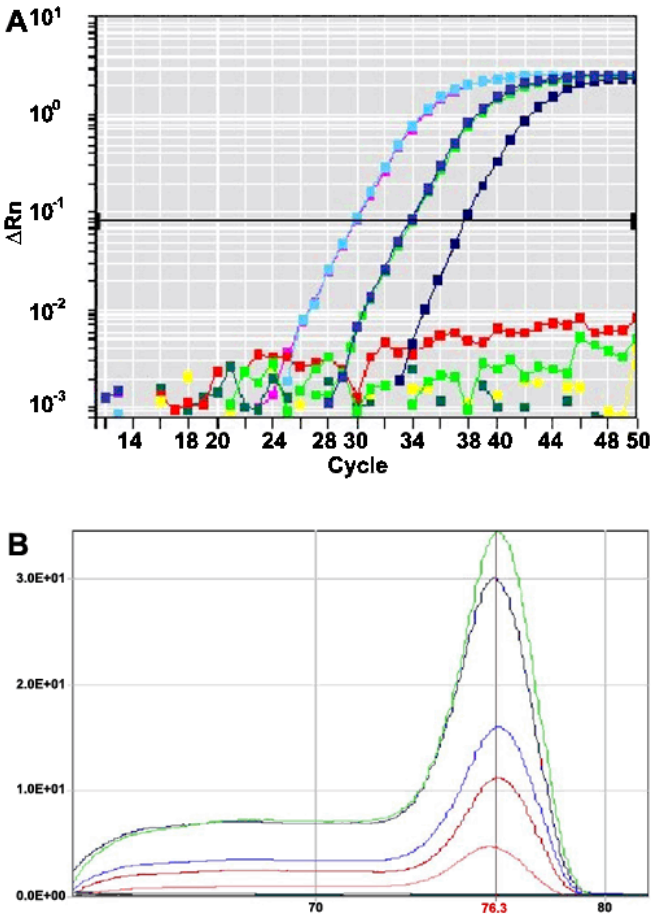

Figure 1. Typical Real-time PCR data. The amplification curves for presenilin 1, obtained with three 10-fold serial dilutions of a cataractous lens-derived cDNA (**A**), and the corresponding melting curves (**B**) are shown. An 80 bp-long amplicon was produced (see Table 2 and Material and Methods for details on Real-Time PCR analysis).

classes was carried out with the EASE program [16]. Lens and human fetal eye EST collections were retrieved from the NEIBank web site.

Real-Time PCR: Real-Time PCR was conducted on reversed-transcribed first strand cDNA derived from the same (N and C1) total RNA samples utilized for microarray hybridization. An independent sample of transparent lens RNA (kindly provided by Marc Kantorow, Department of Biology, University of West Virginia) was utilized as a test RNA to set up Real-Time RT-PCR analysis. Total RNA (1 μg in a final reaction mixture volume of 20 μl) was used for cDNA synthesis, which was carried out at 42 °C for 90 min, followed by thermal inactivation of reverse transcriptase (70 °C for 10 min). All other reaction conditions were the same as those described previously for probe preparation. Real-Time-PCR was performed with a TaqMan ABI PRISM 7700 Sequence Detector System (PE Applied Biosystems, Foster City, CA) according to the manufacturer's instructions. Reaction mixtures (25 μl final volume) were assembled with the following components: 2.5 μl of 10-fold serial dilutions of the two cDNAs, individually optimized amounts of each primer set (300 nM for GCS1 and POLR2E, 50 nM for all the other amplifications), 2X SYBR Green PCR Master Mix (PE Applied Biosystems), containing AmpliTaq GOLD® DNA Polymerase, reaction buffer, dNTPs, Passive Reference and SYBR Green I. The housekeeping βactin [17] and β-2-microglobulin [18] genes served as independent internal standards. To avoid interference by contaminating genomic DNA, all primers (reported in Table 2) were designed to cross exon-intron boundaries using the Primer Express software (PE Applied Biosystems). β-Actin primers were from PE Appled Biosystems (βactin Control reagents, part number 401846). All primer pairs produced only one amplification band (ranging in size from 50 to 90 bp) when tested in conventional RT-PCR. The specificity of individual Real-Time PCR products was assessed by melting curve analysis [19], carried out immediately after PCR completion following the manufacturer's instructions. Melting curves for individual PCR products displayed a single peak. Melting temperatures (Tm) were determined with the Dissociation Curve software (PE Applied Biosystems). All sets of reactions were conducted in triplicate, and each included a non-template control (NTC). A representative amplification plot and the corresponding melting curve are shown in Figure 1. The threshold cycle (Ct) was used to calculate relative gene expression levels using the "Comparative Ct method" (PE Applied Biosystems, User Bulletin number 2), which is based on the assumption that the efficiency of amplification of target and reference cDNAs are approximately the same. The validity of the above assumption was verified for each primer set using serial cDNA dilutions.

Table 3. Comparison between microarray hybridization and lens EST data

	EST Library		
	NEIBank human lens cDNA library	dbEST human lens cDNA library	dbEST human fetal eye
Flag 0	23%	22%	12%
Flag 2	15%	15%	11%
Flag 3	22%	20%	11%

Unigene sequences in the GF211 filter, concordantly flagged in two independent normal lens epithelim (N-probe) hybridizations (see Materials and Methods, and Table 1 for details), were compared with unigene lens ESTs from the NEIBank (2,275 entries) and from the dbEST (2,329) Humal Lens cDNA libraries. A human fetal eye EST database (11,029 unigene sequences) was used as reference for this comparison. Since different numbers of ESTs are available in the different databases, the number of matches obtained from individual pairwise comparisons was normalized with respect to the lowest number of ESTs (2,275), as found in the NEIBank cDNA library.

RESULTS & DISCUSSION

Overall representation of lens epithelium-expressed genes in the microarray: The GF211 microarray utilized in the present study contains cDNAs from various human cDNA libraries, none of which was of lens origin. Therefore, we initially looked for some basic information regarding the proportion of lens-expressed genes that were represented in the GF211 array. To this end, we determined the number of spotted cDNAs with a unigene code (a total of 3,983 entries) that match sequences previously isolated as lens ESTs (NEIBank Human Lens cDNA library [20], 2,275 distinct unigene codes; dbEST Human Lens cDNA library, 2,319 distinct unigene codes). We found that 531 (23.3%) and 555 (23.9%) lens ESTs from such databases match cDNA sequences that are present in the GF211 array. To compare expression levels in transparent human lenses deduced from either EST sampling or cDNA hybridization, we determined the number of sequence matches found in each of our three flag classes. As shown in Table 3, using aggregate concordant data from two independent "normal lens" hybridizations, we found that the percentage of

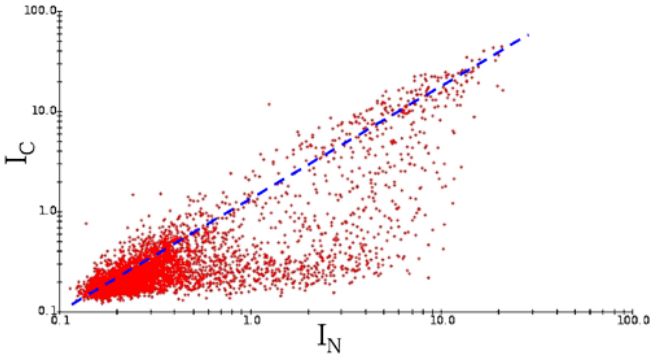

Figure 2. Representative scatterplot of the signal intensities derived from an N versus C comparison. The data shown are from hybridizations conducted with filter 2. Normalized signal intensity calculations and graph construction were performed with the Pathways 4 program. Dots lying above and below the blue dashed line ($I_C/I_N=1$) correspond to normalized signal intensities that are, respectively, higher and lower in cataractous than in transparent lens.

Table 4. Genes differentially expressed in cataractous lens epithelia compared to transparent epithelia

Downregulated genes

Accession number	Title	Gene	Chromosome	Flag N1/N2	I_N	Flag C1/C2	I_C	I_N/I_C
AA291490	glucosidase I	GCS1	2	0/0	3.29	2/2	0.20	16.29
H53703	growth factor receptor-bound protein 7	GRB7	17	0/0	2.43	2/2	0.20	12.06
AA701860	follistatin	FST	5	0/0	2.07	2/2	0.20	10.24
AA027042	Pol (RNA) II (DNA directed) polypeptide E	POLR2E	19	0/0	2.06	2/2	0.20	10.20
AA454218	TBP associated factor.RNA polI.C	TAF1C	16	0/0	1.92	2/2	0.20	9.51
AA443547	v-rel avian reticuloendotheliosis viral oncogene	RELA	11	0/0	1.85	2/2	0.20	9.16
AA147640	phosphorylase, glycogen	PYGL	14	0/0	1.72	2/2	0.20	8.54
T72202	signal transducer and activator of transcription 6	STAT6	12	0/0	1.57	2/2	0.20	7.78
N64051	Werner syndrome	WRN	8	0/0	1.53	2/2	0.20	7.59
AA164440	pericentriolar material1	PCM1	8	0/0	1.51	2/2	0.20	7.50
N81029	collagen, type XVIII, alpha 1	COL18A1	21	0/0	1.49	2/2	0.20	7.39
AA430512	serine (or cysteine) proteinase inhibitor	SERPINB9	6	0/0	1.49	2/2	0.20	7.37
AA463924	coagulation factor VIII-associated	F8A	X	0/0	2.33	0/2	0.32	7.33
AA884403	cardiotrophin 1	CTF1	16	0/0	1.44	2/2	0.20	7.15
AA099169	phosphofructokinase	PFKM	12	0/0	1.42	2/2	0.20	7.06
AA443039	heat shock 70 kD protein 1B	HSPA1B	6	0/0	1.42	2/2	0.20	7.02
AA454854	amylase, alpha 2A	AMY2A	1	0/0	1.38	2/2	0.20	6.85
H79353	Fc fragment of IgE	FCER1G	1	0/0	1.35	2/2	0.20	6.66
AA644128	nuclear autoantigenic protein (histone-binding)	NASP	1	0/0	1.31	2/2	0.20	6.51
AA134814	TRAF family member-associated NFKB activator	TANK	2	0/0	1.29	2/2	0.20	6.41
T55558	colony stimulating factor 1	CSF1	1	0/0	1.28	2/2	0.20	6.34
AA488622	signal transducing adaptor moleculeSH3 domain	STAM	10	0/0	1.28	2/2	0.20	6.32
R44005	glutamate decarboxylase2	GAD2	10	0/0	1.26	2/2	0.20	6.26
AA877347	putative b.b-carotene-9', 10'-dioxygenase	B-DIOX-II	11	0/0	1.25	2/2	0.20	6.18
AA844124	Homo sapiens, clone IMAGE:4070070		14	0/0	1.24	2/2	0.20	6.13
AA496792	ESTs		9	0/0	1.22	2/2	0.20	6.03
AA127100	ribophorin I	RPN1	3	0/0	1.21	2/2	0.20	6.00
AA431795	hypothetical protein EDAG-1	EDAG-1	9	0/0	1.21	2/2	0.20	6.00
AA449753	capping protein (actin filament) muscle Z-line, alpha 1	CAPZA1	1	0/0	1.18	2/2	0.20	5.83
AA401972	RAB2, member RAS oncogene family-like	RAB2L	6	0/0	1.71	0/2	0.31	5.53
AA427906	beclin 1	BECN1	17	0/0	1.11	2/2	0.20	5.49
AA421783	zinc finger protein 263	ZNF263	16	0/0	1.11	2/2	0.20	5.49
AA478724	insulin-like growth factor binding protein 6	IGFBP6	12	0/0	1.11	2/2	0.20	5.48
AA458630	renin	REN	1	0/0	1.10	2/2	0.20	5.44
AA458982	sodium channel, nonvoltage-gated 1 alpha	SCNN1A	12	0/0	1.09	2/2	0.20	5.39
N51278	chemokine (C-X3-C) receptor 1	CX3CR1	3	0/0	1.09	2/2	0.20	5.38

Table 4. continued.

R60150	histidyl-tRNA synthetase	HARS	5	0/0	1.08	2/2	0.20	5.33
AA490855				0/0	1.05	2/2	0.20	5.21
AA488247	amyloid b(A4) precursor protein-binding, family	APBB1	11	0/0	1.43	0/2	0.28	5.21
N23898	G protein-coupled receptor kinase 2 (Drosophila)-like	GPRK2L	4	0/0	1.04	2/2	0.20	5.17
N73499	GTP-binding protein ragB	RAGB	X	0/0	1.02	2/2	0.20	5.05

Upregulated genes

Accession number	Title	Gene	Chromosome	Flag N1/N2	I_N	Flag C1/C2	I_C	I_N/I_C
H72028	gelsolin (amyloidosis, Finnish type)	GSN	9	2/2	0.21	0/0	1.32	6.38
AA293653	phosphoprotein enriched in astrocytes 15	PEA15	1	2/2	0.21	0/0	1.22	5.92
AA504656	latent transforming growth factor β–binding protein 1	LTBP1	2	2/2	0.21	0/0	1.12	5.42
AA070226	selenoprotein P, plasma,1	SEPP1	5	2/2	0.21	0/0	0.99	4.72
AA487460	dihydropyrimidinase-like2	DPYSL2	8	2/2	0.21	0/0	0.71	3.40

Cataract downregulated and upregulated genes (corresponding to flag 0 or flag 2 spots) with a greater than or equal to 5- or 3-fold variation, respectively, are listed in a decreasing order of fold-variation. The complete list of modulated genes is given in Appendix 1.

cDNA sequences with a match in the two lens EST collections was higher for regular (flag 0) and irregular (flag 3) spot classes than for background level (flag 2) spots (see Materials and Methods for "flag" definitions and other experimental details). By comparison, a nearly flat distribution of EST-matching sequences in the various flag classes, was observed when using the dbEST Human Fetal Eye cDNA library as a reference EST database (Table 3). Thus, there seems to be a specific EST enrichment in hybridizing spots tagged as flag 0 and, somewhat unexpectedly, also in flag 3 spots (see below). Flag 2 spots, which represent the most populated flag class in the entire array, comprise, instead, the lowest proportion of EST matching cDNAs. The fact that these sequences have been sampled as ESTs, yet correspond to hybridization-negative spots in our array, might be due to intrinsic technical differences between the two methods. It should also be noticed, however, that at variance with our cDNA probes, which were derived from pure "fiber-free" lens epithelium tags, lens ESTs were sampled from a total lens library, that likely includes sequences of fiber origin. So, even though flag 2 spots are likely to contain a number of lens-expressed genes, they were regarded, in the present study, as representative of genes that are not expressed. A final note regards flag 3 spots, which were thus tagged by the ImaGene program because of their exceedingly large (or irregular) size and consequent difficulty of measuring reliable local background intensity values, yet comprise some of the most strongly hybridizing cDNAs (including, for example, αB-crystallin). Spots tagged as flag 3 in both N probe hybridizations as well as flag 3/flag 0 spot pairs were thus included in the final dataset of lens-expressed genes. This set contains a total of 612 cDNA sequences (Appendix 1), and includes 375 genes that have not yet been sampled as lens ESTs (for example, γA-crystallin). As revealed by a functional classification comparison carried out with the "Molecular function", "Biological process", and "Cellular component" categories of GeneOntology [14], there was a substantial overlap between the distribution of the total ensemble of arrayed cDNAs among different functional classes and the corresponding distribution of the subset of cDNAs that we found to be expressed in the lens epithelium. The only notable exceptions are genes belonging to the classes "Protein phosphatase" (n=8), "Base-excision repair" (n=5), "Chaperone activity" (n=13), "EGF receptor signalling" (n=4), and "Oxygen and reactive oxygen species metabolism" (in particular, the "Response to oxidative stress" subclass; n=7). All of these classes are significantly more represented (Fisher's Exact Test, $P<0.05$) in the expressed cDNAs than in the ensemble of filter-arrayed cDNAs.

Differential mRNA expression profiles in transparent and nuclear cataractous lenses: Having defined a subset of arrayed cDNAs that have expressed counterparts in the mRNA population of human lens epithelia, we set out to compare the expression profiles of transparent lens epithelia (N) with those of epithelial tags sampled from two separate groups of patients (of closely matching sex and age) affected by nuclear age-related cataract (C). A representative scatter plot derived from an N versus C comparison is shown in Figure 2. What is readily apparent is that most of the dots deviating from the diagonal, lie in a region of the diagram where the I_C/I_N signal intensity ratio is lower than one. This suggests that an extensive downregulation is the main gene expression change associated with cataract formation. A more rigorous data analysis, based on the above described flagging criteria (see Materials and Methods for details), was then conducted on hybridizations performed with the same filter (N1 versus C1 and N2 versus C2) as well as across filters (N1 versus C2 and N2

versus C1). Only spots giving consistent results across all four comparisons, with an average signal intensity ratio greater than or equal to 2.5, were deemed as modulated. By applying the above criteria, we found that 269 mRNAs appeared to be modulated, 262 were downregulated in cataractous epithelia compared to epithelia from transparent lenses, while the remaining seven mRNAs were upregulated in cataracts. Cataract-downregulated and upregulated mRNAs with a greater than or equal to 5.0 fold-variation are listed in Table 4. The entire dataset, filtered to accommodate the above requirements, is provided in Appendix 1.

Table 5. Validation of a subset of modulated genes by Real-Time PCR

Gene	N/C Fold Change	
	Microarray	Real-Time PCR
Glucosidase I	16.3	35.5
Polymerase (RNA) II, polypeptide E	10.2	2.9
Presenilin I	4.7	2.1
Crystallin βA4	5.4	6.8
Gelsolin	0.16	2.0
Dihydropyrimidinase-like 2	0.29	0.11

Microarray data were derived from four N versus C hybridization comparisons as specified in the text (see also Table 4). Real-Time PCR data were obtained with the Comparative Ct method (see Materials and Methods and Table 2 for details on Real-Time PCR experiments and amplification primers).

Two of the most downregulated mRNAs (glucosidase I and RNA pol II polypeptide E), an mRNA of intermediate downregulation (presenilin I), all identified by flag 0 spots, and a downregulated mRNA (βA4-crystallin), identified by a flag 3 spot, were chosen as candidate sequences for an independent verification of microarray data, together with two upregulated genes (gelsolin and dihydropyrimidinase-like 2), both identified by flag 0 spots. This was conducted with Real-Time PCR using both βactin and β2-microglobulin as internal standards and the "Comparative Ct method" to calculate relative gene expression levels (see Materials and Methods for details). As shown in Table 5, even though quantitative variations between the two methods can be as high as 3.5-fold, Real-Time PCR results confirmed microarray data for all tested genes, except gelsolin.

Functional classification and possible cataract-disease significance of differentially expressed genes: The overall distribution of the 262 cataract-downregulated genes within different categories of the GeneOntology classification system (the "Biological process" and "Cellular component" catego-

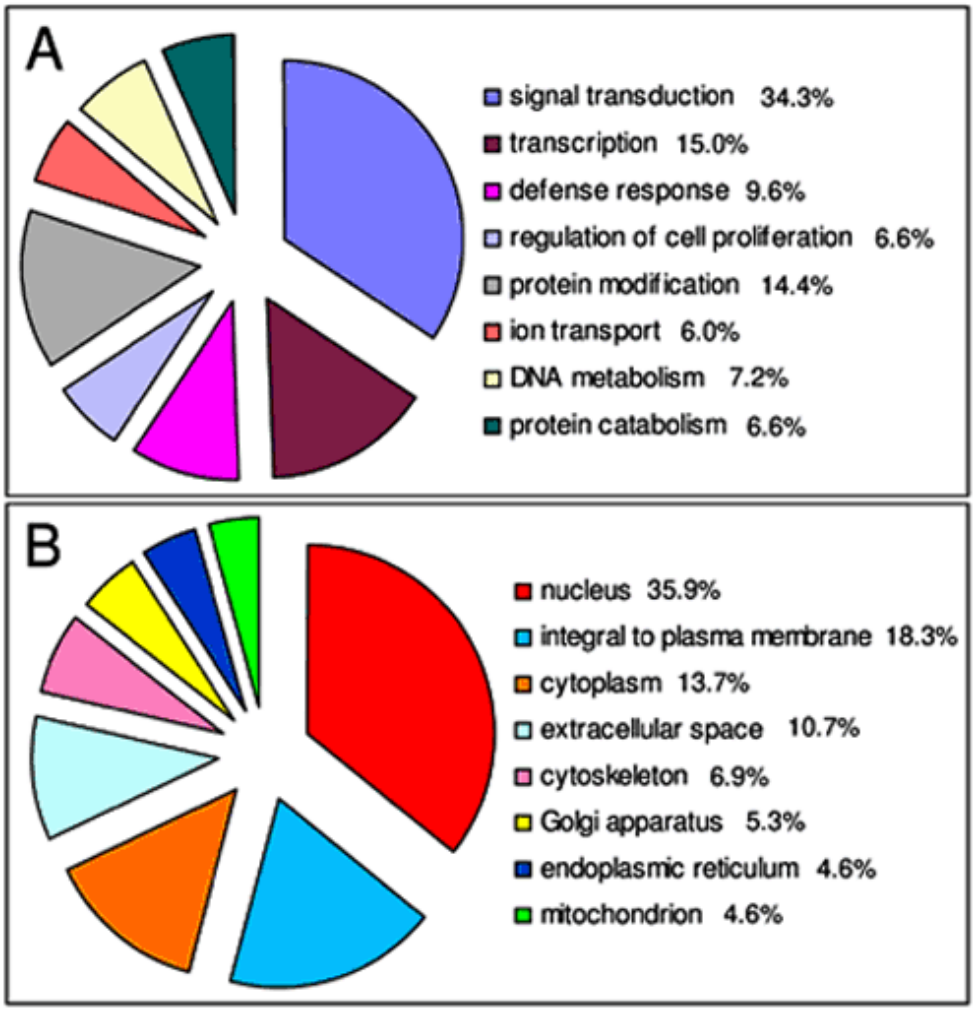

Figure 3. Distribution of cataract-downregulated genes in different Gene Ontology categories. Pie chart showing the distribution of cataract-downregulated genes in the "Biological process" (A) and "Cellular component" (B) functional categories of the Gene Ontology classification [14]. Only the eight most populated classes are shown. The total number of genes shown in (A) and (B) is 166 and 131, respectively; the percentage of genes in each class is indicated in the inset legend.

ries) overlaps quite closely the corresponding distribution of the total set of lens epithelium-expressed genes (Figure 3). A few notable exceptions, however, were found for gene classes, such as "Signal transduction" (in particular, for the "EGF receptor signalling" subclass), "Regulation of cell proliferation", and "Protein modification", whose relative content in cataract-downregulated genes was significantly higher (Fisher's Exact Test; $P<0.05$) than that expected on a purely statistical basis. Such classes, which can be regarded as representative of preferential targets of the generalized downregulation that accompanies cataract formation, are shown in Figure 4. Also shown in Figure 4 are some of the classes that displayed the opposite trend, ie a relative abundance in cataract-downregulated genes significantly lower than expected. Interestingly, these include some of the classes, such as the "Response to oxidative stress" class, that were previously found to contain a disproportionately high number of lens expressed genes. These classes can thus be viewed as representative of groups of genes whose mRNA output is kept at nearly constant levels even in cataractous lenses.

We also examined classes with a high absolute content of cataract-downregulated genes, regardless of how the number of such genes compares with the total number of lens-expressed genes belonging to that particular class (Figure 3). Among the most populated, there are the classes "Integral to plasma membrane" (n=28) and "Transcription" (n=25). The latter class includes various transcription factors and other transcription-related proteins, such as the RNA polymerase II polypeptides E and G, the MADS Box Transcription Enhancer Factor 2, the cAMP Response Element Binding Protein, the Retinoic Acid Receptor alpha, the Zinc-finger proteins 137 and 263, the TATA box-Binding Protein associated factor TAF1C, Transcription Factor IIIA, and the RNA polymerase III subunit RPC8. Also notable is the presence among the most downregulated mRNAs (Table 4) of three transcripts (RelA, TANK and CSF1) coding for proteins that are functionally related to NFkB, a transcription factor known to play important roles in stress, inflammation, and ageing [21]. In the class "Integral to plasma membrane", the presenilin 1 and presenilin 2 mRNAs were both appreciably downregulated and a similar downregulation was observed for the amyloid βprecursor binding proteins APBB1 and APBA2. Presenilins are key components of the secretase multiprotein complexes that are responsible for Alzheimer precursor protein (AβPP) processing, and generation of the cytotoxic β-amyloid polypeptide (Aβ). Both presenilins are known to be expressed in the lens, where the Aβ-polypeptide has been shown to accumulate in the lens epithelia of both Alzheimer and non-Alzheimer patients [22-25]. The findings regarding the downregulation of the presenilin and APBB mRNAs, as well as the downregulation of a number of chaperone and chaperone-like protein mRNAs (see below), may be relevant to our problem, as it is known that Aβ is highly toxic for lens epithelial cells, it increases in the lens following oxidative stress [22] and, in Alzheimer disease, it is deposited in the lens and colocalizes in plaques along with HSP27 and αB-crystallin [23,24].

Other mRNAs that are strongly downregulated in cataractous lenses (Table 4 and Appendix 1) are potentially interesting. Besides glucosidase 1, an enzyme involved in the quality control processing of N-glycosylated polypeptides and belonging to the "Protein modification" class, these include, for example, βA4-crystallin, the heat shock proteins 70kD 1B

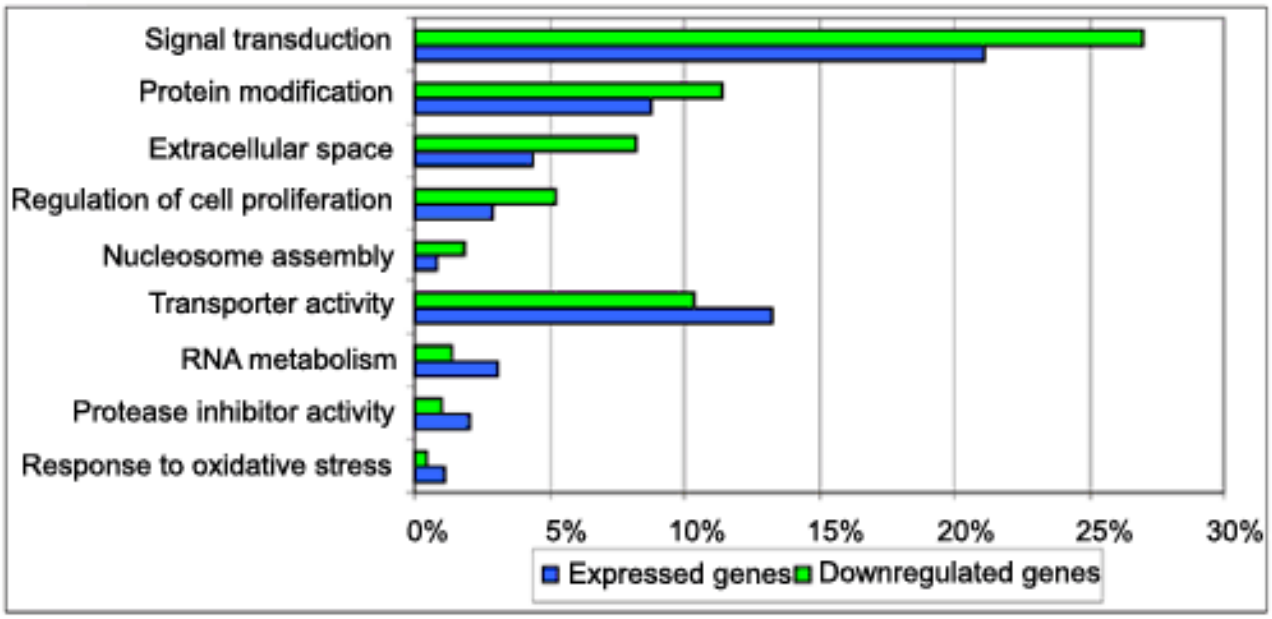

Figure 4. Comparative distribution of lens-expressed and cataract-downregulated genes within different functional classes. The histogram shown, represents a subset of Gene Ontology classes (from the "Biological process", "Cellular component" and "Molecular function" categories [14]), in which the number of downregulated genes is significantly higher (the five top sets of bars) or lower (the four bottom sets of bars) than expected (Fisher's Exact Test, $P<0.05$). The x-axis represents the percentage of genes within each functional class. Lens-expressed gene classes are indicated by blue bars; cataract-downregulated gene classes are indicated by green bars.

and 27kD 2, the ubiquitin-conjugating enzymes E2E 1 and E2A, and the Werner Syndrome polypeptide, a molecular marker of a complex disease characterized by precocious aging and early onset cataract. βA4-crystallin has been found to represent the sixth most abundant EST in an adult human lens library [20], and its marked downregulation in cataracts contrasts with the lack of a consistent expression change observed for five other crystallins (αA-, αB-, βA3/A1-, γA-, and γC-crystallin). Among molecular chaperones, the heat-shock proteins hsp70 and hsp27, were consistently downregulated in cataracts. Two other downregulated transcripts, belonging to the "Cytoskeleton" class (n=18), code for the α1 and β5 subunits of tubulin, a microtubule protein that resembles molecular chaperones in its ability to suppress the aggregation of various proteins including soluble lens proteins such as β- and γ-crystallins [26].

Translation-related genes such as those coding for ribosomal protein RPS4Y, ribosomal protein chinase RPS6KB1, the translation initiation factor EIF4G3, and histidyl-tRNA synthetase were also found to be downregulated. To these must be added the previously mentioned transcription factor IIIA and RNA polymerase III RPC8 subunit, which are involved in the biosynthesis of key translation components such as 5S rRNA and tRNAs. In keeping with these data, a previous differential display RT-PCR analysis has shown that various ribosomal protein genes appear to be downregulated in human age-related cataract [11]. This suggests that the development of age-related cataract in man is characterized, among other things, by a substantial depression of protein biosynthesis. On a similar note, Kantorow et al. [10] reported a decreased expression of the protein Phosphatase 2A regulatory subunit mRNA in the lens epithelium of human age-related cataracts. We had for this gene inconsistent results, but observed a reproducible downregulation of the phosphatase 2 regulatory subunit B and phosphatase 1 regulatory subunit 7 mRNAs.

Glutathione S-transferase A4 was one of the few downregulated genes belonging to the "Oxygen and reactive oxygen species metabolism" class. No modulation was detected for other anti-oxidative defense genes such as glutathione reductase, superoxide dismutase, peroxidase, and catalase. Interestingly, Goswami et al. [27] reported an increased expression of glutathione S-transferase θ2 following in vitro exposure of human lens epithelial cells to 50 μM H_2O_2, and Spector et al. [28] found several members of the Glutathione S-transferase family to be upregulated in mouse lens epithelial cell lines conditioned to survive peroxide stress.

A final note regards the seven mRNAs that we found to be upregulated in cataract (Table 4). If one considers their small number, which strikingly contrasts with the 262 downregulated genes, it is not so surprising that such genes also turned out to be less reliable in terms of Real Time PCR confirmation. In fact, the finding of some false positives is not an uncommon occurrence in analyses dealing with thousands of genes. Assuming that false positives are not due to a systematic error, they should be randomly distributed between up- and downregulated genes. Thus, considering our limited number of upregulated genes, the finding of a gene whose upregulation was not confirmed by Real-Time-PCR analysis is not unexpected.

Conclusions: Knowledge of the changes in gene expression that accompany the development of human cataract may contribute to a better understanding of the opacification process. In this study, we have utilized DNA microarrays to compare the expression profiles of 4,132 known human genes in the central lens epithelium of normal and cataractous human lenses. We have limited our analysis to cataracts with a clinically significant N opacity and absent or minimal C and/or PSC components (less than or equal to 1 according to the LOCS II severity scale). The data indicate that the response of the lens epithelium to the development of age-related nuclear cataract is characterized by an extensive downregulation.

Our study has some limitations, including the relatively limited number of genes tested (only about 12% of the estimated protein coding gene complement of the human genome) and the fact that only RNA samples from the central part of the lens epithelium were utilized for hybridizations. It also has some strengths, however, such as the careful slit-lamp classification of the type and severity of cataracts (and thus the fact that the cataractous lens population we analyzed is representative of a specific type of opacity), the microsurgical technique utilized for the preparation of epithelial capsule tags from transparent control lenses, and their relatively good age matching with cataract samples. Even though the data were derived from the analysis of a specific portion of the lens epithelium, it is likely that the downregulation response we have identified applies to the whole lens epithelium as well. This response differs considerably from that observed by Goswami et al. [27] in cultured human lens epithelial cells exposed to an acute, H_2O_2-induced oxidative stress, in which mRNA upregulation substantially exceeded downregulation. Interestingly, however, differential expression profiles characterized by an extensive downregulation, similar to the one we have documented here, have been reported previously for other age-related diseases, most notably Alzheimer. Using DNA microarrays containing 12,633 ESTs to compare the gene expression pattern of hippocampal tissue from Alzheimer disease with that of control patients, Colangelo et al. [29] found that Alzheimer brain shows a generalized downregulation in gene transcription, which includes transcription factors, neurotrophic factors and synaptic plasticity-related genes. Similarly, in a microarray gene expression analysis in a transgenic *Caenorhabditis elegans* Alzheimer's disease model, Link et al. [30] found 6 upregulated and 240 downregulated genes. So, even though the possibility that a transiently increased expression of specific (eg, cellular defense) genes may take place at the very onset of cataractogenesis cannot be excluded, it is tempting to speculate that age-related diseases, including cataract, are characterized by a tendency towards the shut down of de novo RNA and protein biosynthesis, rather than by the upregulation of cell defense components, such as chaperones and various kinds of antioxidative or detoxifying proteins.

ACKNOWLEDGEMENTS

We thank Mark Kantorow (Department of Biology, Univer-

sity of West Virginia) for the gift of a transparent lens RNA sample, Tauro Neri (Molecular Genetics and Diagnostic Biotechnologies, University of Parma) for sharing Real-Time PCR instrumentation, and Stefania Petrucco and Chiara Chiapponi (Department of Biochemistry and Molecular Biology, University of Parma) for help in an early phase of this work. This work was supported in part by University of Parma FIL grants 2002 and 2003 (G.M. and S.O.) and by the FIRB program "Post-genome: Cellular Physiology and Engineering" (Ministry of education, University and Research, to S.O.).

REFERENCES

1. Spector A. Oxidative stress-induced cataract: mechanism of action. FASEB J 1995; 9:1173-82.
2. Spector A, Garner WH. Hydrogen peroxide and human cataract. Exp Eye Res 1981; 33:673-81.
3. Li WC, Kuszak JR, Dunn K, Wang RR, Ma W, Wang GM, Spector A, Leib M, Cotliar AM, Weiss M. Lens epithelial cell apoptosis appears to be a common cellular basis for non-congenital cataract development in humans and animals. J Cell Biol 1995; 130:169-81.
4. Harocopos GJ, Alvares KM, Kolker AE, Beebe DC. Human age-related cataract and lens epithelial cell death. Invest Ophthalmol Vis Sci 1998; 39:2696-706.
5. Leske MC, Chylack LT Jr, Wu SY. The Lens Opacities Case-Control Study. Risk factors for cataract. Arch Ophthalmol 1991; 109:244-51.
6. Vitale S, West S, Hallfrisch J, Alston C, Wang F, Moorman C, Muller D, Singh V, Taylor HR. Plasma antioxidants and risk of cortical and nuclear cataract. Epidemiology 1993; 4:195-203.
7. Risk factors for age-related cortical, nuclear, and posterior subcapsular cataracts. The Italian-American Cataract Study Group. Am J Epidemiol 1991; 133:541-53.
8. Sheets NL, Chauhan BK, Wawrousek E, Hejtmancik JF, Cvekl A, Kantorow M. Cataract- and lens-specific upregulation of ARK receptor tyrosine kinase in Emory mouse cataract. Invest Ophthalmol Vis Sci 2002; 43:1870-5.
9. Kantorow M, Horwitz J, Carper D. Up-regulation of osteonectin/SPARC in age-related cataractous human lens epithelia. Mol Vis 1998; 4:17 .
10. Kantorow M, Kays T, Horwitz J, Huang Q, Sun J, Piatigorsky J, Carper D. Differential display detects altered gene expression between cataractous and normal human lenses. Invest Ophthalmol Vis Sci 1998; 39:2344-54.
11. Zhang W, Hawse J, Huang Q, Sheets N, Miller KM, Horwitz J, Kantorow M. Decreased expression of ribosomal proteins in human age-related cataract. Invest Ophthalmol Vis Sci 2002; 43:198-204.
12. Wilson AS, Hobbs BG, Speed TP, Rakoczy PE. The microarray: potential applications for ophthalmic research. Mol Vis 2002; 8:259-70 .
13. Chylack LT Jr, Leske MC, McCarthy D, Khu P, Kashiwagi T, Sperduto R. Lens opacities classification system II (LOCS II). Arch Ophthalmol 1989; 107:991-7.
14. Ashburner M, Ball CA, Blake JA, Botstein D, Butler H, Cherry JM, Davis AP, Dolinski K, Dwight SS, Eppig JT, Harris MA, Hill DP, Issel-Tarver L, Kasarskis A, Lewis S, Matese JC, Richardson JE, Ringwald M, Rubin GM, Sherlock G. Gene ontology: tool for the unification of biology. The Gene Ontology Consortium. Nat Genet 2000; 25:25-9.
15. Dennis G Jr, Sherman BT, Hosack DA, Yang J, Gao W, Lane HC, Lempicki RA. DAVID: Database for Annotation, Visualization, and Integrated Discovery. Genome Biol 2003; 4:P3.
16. Hosack DA, Dennis G Jr, Sherman BT, Lane HC, Lempicki RA. Identifying biological themes within lists of genes with EASE. Genome Biol 2003; 4:P4.
17. Kreuzer KA, Lass U, Landt O, Nitsche A, Laser J, Ellerbrok H, Pauli G, Huhn D, Schmidt CA. Highly sensitive and specific fluorescence reverse transcription-PCR assay for the pseudogene-free detection of beta-actin transcripts as quantitative reference. Clin Chem 1999; 45:297-300.
18. Vandesompele J, De Preter K, Pattyn F, Poppe B, Van Roy N, De Paepe A, Speleman F. Accurate normalization of real-time quantitative RT-PCR data by geometric averaging of multiple internal control genes. Genome Biol 2002; 3:RESEARCH0034.
19. Ririe KM, Rasmussen RP, Wittwer CT. Product differentiation by analysis of DNA melting curves during the polymerase chain reaction. Anal Biochem 1997; 245:154-60.
20. Wistow G, Bernstein SL, Wyatt MK, Behal A, Touchman JW, Bouffard G, Smith D, Peterson K. Expressed sequence tag analysis of adult human lens for the NEIBank Project: over 2000 non-redundant transcripts, novel genes and splice variants. Mol Vis 2002; 8:171-84 .
21. Li X, Stark GR. NFkappaB-dependent signaling pathways. Exp Hematol 2002; 30:285-96.
22. Frederikse PH, Garland D, Zigler JS Jr, Piatigorsky J. Oxidative stress increases production of beta-amyloid precursor protein and beta-amyloid (Abeta) in mammalian lenses, and Abeta has toxic effects on lens epithelial cells. J Biol Chem 1996; 271:10169-74.
23. Liang JJ. Interaction between beta-amyloid and lens alphaB-crystallin. FEBS Lett 2000; 484:98-101.
24. Goldstein LE, Muffat JA, Cherny RA, Moir RD, Ericsson MH, Huang X, Mavros C, Coccia JA, Faget KY, Fitch KA, Masters CL, Tanzi RE, Chylack LT Jr, Bush AI. Cytosolic beta-amyloid deposition and supranuclear cataracts in lenses from people with Alzheimer's disease. Lancet 2003; 361:1258-65.
25. Li G, Percontino L, Sun Q, Qazi AS, Frederikse PH. Beta-amyloid secretases and beta-amyloid degrading enzyme expression in lens. Mol Vis 2003; 9:179-83 .
26. Guha S, Manna TK, Das KP, Bhattacharyya B. Chaperone-like activity of tubulin. J Biol Chem 1998; 273:30077-80.
27. Goswami S, Sheets NL, Zavadil J, Chauhan BK, Bottinger EP, Reddy VN, Kantorow M, Cvekl A. Spectrum and range of oxidative stress responses of human lens epithelial cells to H2O2 insult. Invest Ophthalmol Vis Sci 2003; 44:2084-93.
28. Spector A, Li D, Ma W, Sun F, Pavlidis P. Differential amplification of gene expression in lens cell lines conditioned to survive peroxide stress. Invest Ophthalmol Vis Sci 2002; 43:3251-64.
29. Colangelo V, Schurr J, Ball MJ, Pelaez RP, Bazan NG, Lukiw WJ. Gene expression profiling of 12633 genes in Alzheimer hippocampal CA1: transcription and neurotrophic factor down-regulation and up-regulation of apoptotic and pro-inflammatory signaling. J Neurosci Res 2002; 70:462-73.
30. Link CD, Taft A, Kapulkin V, Duke K, Kim S, Fei Q, Wood DE, Sahagan BG. Gene expression analysis in a transgenic Caenorhabditis elegans Alzheimer's disease model. Neurobiol Aging 2003; 24:397-413.

Appendix 1. List of lens expressed and modulated genes

This appendix includes two files containing separate lists for genes that are expressed in the human lens ("gene-expressed.txt") or modulated in cataractous versus transparent lenses ("gene-modulated.txt").

The file "gene-expressed.txt" contains the list of genes corresponding to spots with "above-background" hybridization signals in transparent human lenses (see the text for details on data analysis). Columns correspond to: (1) GenBank accession number, (2) GenBank gene definition, (3) Gene symbol, (4) flags for "normal lens" hybridization on filter 1 (N1) and for "normal lens" hybridization on filter 2 (N2) as assigned by the Imagene data analysis software (see Methods for details), (5) average of normalized signal intensities obtained from "normal lens" hybridizations conducted on filter 1 and filter 2, and (6) presence in (yes), or absence from (no) lens Expressed Sequence Tag (EST) collections for all hybridization-positive genes identified by our analysis. Flag 0 spots were normalized with respect to the mean of all the hybridization intensities of flag 0 spots. Spots to which a flag 3 was assigned in at least one hybridization were normalized with respect to the mean intensity of all "above-background" spots.

The file "gene-modulated.txt" contains the list of genes that are differentially expressed in transparent versus nuclear cataractous lenses (see the text for details on data analysis). Columns correspond to: (1) GenBank accession number, (2) GenBank gene definition, (3) Gene symbol, (4) flags for "normal lens" hybridization on filter 1 (N1) and for "normal lens" hybridization on filter 2 (N2) as assigned by the Imagene data analysis software (see Methods for details), (5) flags for "cataractous lens" hybridization on filter 1 (C1) and for "cataractous lens" hybridization on filter 2 (C2) as assigned by the Imagene data analysis software, and (6) ratio between the average of normalized signal intensities for "normal lens" hybridizations (IN) and the average of normalized signal intensities for "cataractous lens" hybridizations (IC). Flag 0 spots were normalized with respect to the mean of all the hybridization intensities of flag 0 spots. Spots to which a flag 3 was assigned in at least one hybridization were normalized with respect to the mean intensity of all "above-background" spots.

To access this data, click or select the words "normalized data" in the online version of this article. This will initiate the download of a compressed (zip) archive. This file should be uncompressed with an appropriate program (the particular program will depend on your operating system). Once extracted, you will have a folder (or directory) containing two files. The files are tab delimited text. Most spreadsheet programs will import files in this format.

The print version of this article was created on 7 Oct 2003. This reflects all typographical corrections and errata to the article through that date. Details of any changes may be found in the online version of the article.